

THE 4TH INTERNATIONAL CONFERENCE ON ALUMINUM ALLOYS

BEHAVIOUR AND DAMAGE DEVELOPMENT OF 2024 ALLOY UNDER MULTIAXIAL CYCLIC LOADING

V. Ferney, L. Hautefeuille-Beylat, M. Clavel
Université de Technologie de Compiègne, LG2mS, URA CNRS 1505, B.P. 649, 60206
COMPIEGNE Cedex, FRANCE

Abstract

The objective of this paper is to understand the behaviour and the low-cycle fatigue damage of the 2024 alloy (in both an underaged and overaged state), under multiaxial loading. Under proportional loading, the underaged alloy exhibits very homogeneous deformation modes (prismatic loops). In the overaged alloy, interface dislocations are observed. The overstrengthening induced by an out-of-phase tension-torsion loading proceeds mainly from isotropic hardening. In the underaged state, it is due to Lomer barrier formation. A classical approach, applied to the overaged alloy, leads to values of the hardening, caused by geometrically-necessary dislocations, comparable to experimental results.

As predicted by the literature, non proportional loading affect the life of the specimens. For each test, the density of microcracks versus orientation is measured : cracks are present on the direction perpendicular to the tensile stress for the two types of loading (proportional and non proportional). For non proportional tests however, a significant increase in the microcrack density is observed : at the end of the life, there was no direction without cracking.

Introduction

It is now well established that some metals and alloys exhibit significant hardening effects under non proportional loadings. This phenomenon is closely related to the degree of non proportionality. From a microstructural point of view, these overstrengthening effects are unambiguously associated with the slip system multiplicity. However, the physical bases of the overstrengthening are not yet clearly understood. The slip system multiplicity can produce either an isotropic strengthening (forest hardening) or a kinematic strengthening (back stress hardening) ; most of the authors consider that the overstrengthening results from the isotropic hardening. It would be a very interesting topic to compare the effect of non proportionality on a precipitate strengthened alloy such as 2024, the propensity of which to exhibit kinematic or isotropic hardening may be enhanced by metallurgical heat treatments. After studying the mechanical behaviour of the 2024 as a function of the loading path, we will analyse the crack initiation and growth, and the orientation of crack population, under three types of loading : tension-compression, reversed torsion and out-of-phase tension-torsion.

Material and experimental procedure

Material

The material employed in this investigation is an aluminium alloy, the 2024. Its chemical composition is given in table 1 :

element	Al	Cu	Mg	Mn	Fe	Si	Ti	Cr
weight (%)	base	4.32	1.44	0.64	0.22	0.11	0.04	0.01

Table 1. Chemical composition of the alloy

In this work, the alloy was studied in an underaged state (T4 heat treatment) and an overaged state (T4 + annealing for 4 hours at 190°C). In the underaged (U.A.) state, the presence of GPB zones is expected in agreement with the increase in mechanical properties with prolonged natural ageing. A dispersion of $Al_2Cu_2Mn_3$ particles exhibits the following parameters : 0.08 μm mean diameter, 0.18 μm mean length and 0.3 μm mean interparticle spacing. In the overaged (O.A.) state, there is an abundant precipitation of the S' (Al_2CuMg) phase. This dispersion of S' needles exhibits the following parameters : 3 nm mean diameter, 0.17 μm mean length and 0.1 μm mean interrod spacing. For the two heat treatments, the measured mean grain size was 50 μm .

Experimental procedure

Three types of cyclic tests were carried out at room temperature on a tension-torsion servohydraulic machine, using thin-walled tubes : tension-compression, reversed torsion, and out-of-phase tension-torsion test, with a sinusoidal wave-form, and a phase lag of 90° between the two sinusoidal signals. The imposed Von Mises equivalent plastic strain is the same ($4 \cdot 10^{-3}$) for all the types of tests. For the study of the mechanical behaviour, only tension and tension-torsion tests are presented. For the study of the damage development, biaxial specimens were polished to facilitate the observations of the surface cracking, and to avoid crack initiation on manufacturing stripes.

Cellulose acetate tape replicas were made during testing at periodic intervals. They were observed after the test to analyse the crack initiation and growth, and the orientations of the crack population.

Mechanical behaviour

Experimental results

The evolution of the maximum Von Mises equivalent stress of each cycle (σ_{VMmax}) as a function of the accumulated plastic strain p is shown on figure 1. There is a significant additional hardening effect corresponding to the non proportional loading path. This hardening effect amplitude represents about 12 % in the U.A. state, and about 22 % in the O.A. state.

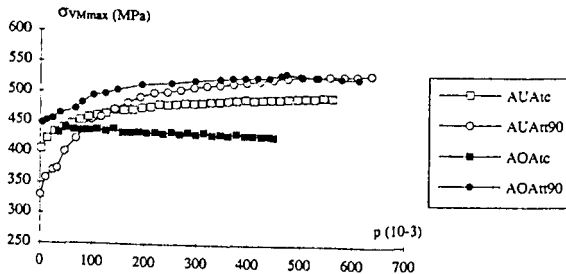


Figure 1. Evolution of the maximum equivalent stress as a function of the accumulated plastic strain

AUAtc : U.A. state, tension test
 AOAtc : O.A. state, tension test

AUAtt90 : U.A. state, out-of-phase tension-torsion test
 AOAtt90 : O.A. state, out-of-phase tension-torsion test

Microstructural observations

In the U.A. alloy, in the case of the tension loading, the deformation substructure observed revealed numerous dislocation loops, and a low dislocation density essentially of screw character, as illustrated on figure 2a.

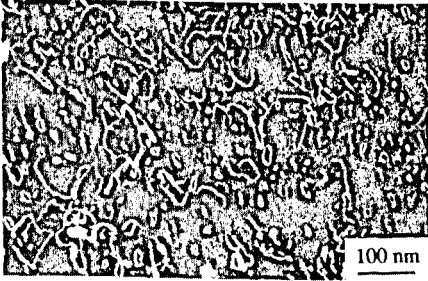


Figure 2a. U.A. state. T.E.M. Weak beam method. Dislocation arrangement created during tension tests : prismatic loops

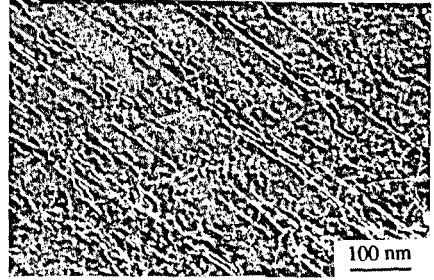


Figure 2b. U.A. state. T.E.M. Weak beam method. Dislocation arrangement created during out-of-phase tests : Lomer locks

These loops were identified as prismatic loops (1). For the nonproportional loading path, numerous dislocation loops were observed, but a particular dislocation structure was also noted, made of straight dislocations lying in the $\langle 110 \rangle$ directions (figure 2b). The identification has shown that these dislocations are Lomer locks (1).

In the O.A. alloy, after tension testing interface dislocations are observed (figure 3a), which are similar to the ones previously observed by Calabrese and Laird (2) in an Al-4Cu under low deformation. After the tension-torsion loading, the interface dislocation network is more complex : it is similar to the one observed by these authors (2) under strong deformation.

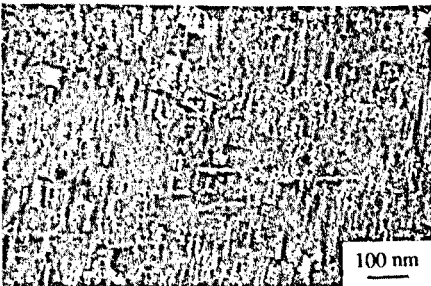


Figure 3a. U.A. state. T.E.M. Weak beam method. Dislocation arrangement created during tension tests : dislocations stored at the S' interfaces, single slip

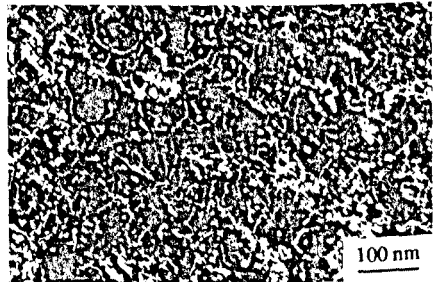


Figure 3b. U.A. state. T.E.M. Weak beam method. Dislocation arrangement created during out-of-phase tests, multiple slip

Discussion

As it was expected, a nonproportional loading path promotes an extra hardening whatever the heat treatment. It should be interesting to appreciate the two components of the strengthening (isotropic and kinematic), as a function of the loading path. Such values were measured from uniaxial hysteresis loops, obtained during tension loading after the steady state,

following a procedure going back to Cottrell (3), and developed by Kuhlmann-Wildsdorf and Laird (4), as indicated on figure 4 (for further details about this procedure, see (5)).

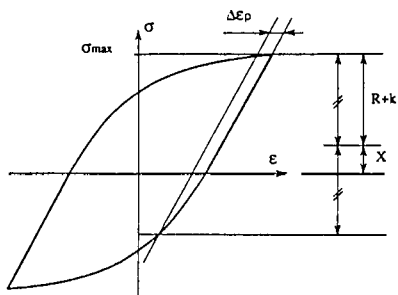


Figure 4. Definition of X and R parameters in an uniaxial fatigue hysteresis loop, from values of the maximum stress σ_{max} , and the yield stress after elastic unloading. The width of the domain of elasticity is defined with a conventional plastic strain of $4 \cdot 10^{-4}$. k is the initial yield stress.

Table 2 shows the main results of strengthening components for the two heat treatments. Results about tension tests (labelled AUAtc and AOAtc) are shown on figure 5.

	Observations	Tests AUAtc and AOAtc	Tests AUAtt90 and AOAtt90
U.A. state k = 370 MPa	Measured values	$\sigma_{max} = 473$ MPa R = -14 MPa X = 117 MPa	$\sigma_{max} = 522$ MPa R = 54 MPa X = 98 MPa
	Microstructural features	homogeneous deformation loops, screw dislocations	homogeneous deformation loops, Lomer locks
O.A. state k = 252 MPa	Measured values	$\sigma_{max} = 423$ MPa R = 33 MPa X = 138 MPa	$\sigma_{max} = 501$ MPa R = 128 MPa X = 121 MPa
	Microstructural features	interface dislocations, single slip	interface dislocations, multiple slip

Table 2. Isotropic and kinematic components of the strengthening, and associated deformation modes

Influence of the heat treatment on the mechanical behaviour

The deformation substructure in the case of a proportional loading of the 2024 in the U.A. state is numerous prismatic loops. In this alloy, Cu and Mg atoms avoid cross slip mechanism favouring planar slip and jog formation on glissile dislocations. Such jogs enhance vacancy formation : loops result from vacancy clustering mechanisms (1). We have already shown that the density of these loops is a function of the cyclic stress (6). Nevertheless, the weak strengthening due to the loops is partly hidden by G.P.B. shearing. On figure 5a, G.P.B. shearing is shown by the negative value of R. The continuous increase in R during the test corresponds to the increase in the loop density. A comparison between the R component and the stress (figure 1) shows that the evolutions of these two parameters are the same : so, the strengthening depends on the density of debris. Figure 5b shows that in the case of the O.A. alloy, the isotropic component is positive and constant during the test. These results are in accordance with the non-shearing of the S' phase, and the absence of debris in the interrod space. In this case, Ashby's approach (7), developed by Calabrese and Laird (2) seems to be appropriate to the 2024.

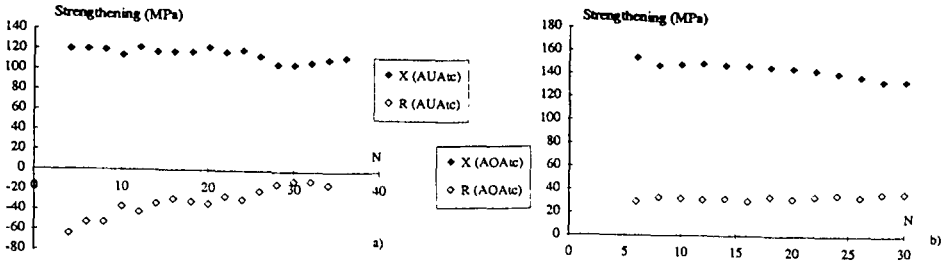


Figure 5. Tension tests. Evolution of the isotropic (R) and kinematic (X) components versus the number of cycles N, for the two heat treatments :
a) U.A. state b) O.A. state

Table 2 shows that, whatever the loading path, the kinematic component is more important in the O.A. alloy than in the U.A. alloy. Even if this result is in accordance with our microstructural observations, a quantitative discussion of these values is too difficult, considering the present knowledge of the behaviour of these substructures.

Influence of the loading path on the strengthening

As shown in table 2, for the two heat treatments, the cyclic stress difference between tension and out-of-phase tension-torsion tests originates mainly from the isotropic component. In the U.A. state, Lomer locks, which come from slip system interactions, are created ; then out-of-phase test microstructure appears as a mixture of numerous dislocation loops and Lomer locks. The presence of these two configurations corresponds with an increase in the slip multiplicity. This result is in accordance with a numerical simulation (8), which shows a multiplication by a factor 1.6 of the number of slip systems. So, the strengthening observed is a forest hardening : Lomer locks act as slight barriers ; they have previously been considered as line like obstacles (9), with a weak strengthening expected.

In the O.A. alloy, the deformation modes are dependant of the precipitation of the S' phase. S' can be considered as a non shearable phase, which is in accordance with the positive value of the isotropic component. The presence of interface dislocations is proof of S'/matrix deformation incompatibilities. The density of geometrically necessary dislocations can be calculated, and we can estimate how many dislocations glide in a cubic box defined by adjacent precipitates (for further details, see Ferney et al. (10)). For an average cell of 10^{-14} m^2 , approximately 8 dislocations only are needed to account for the strain. This result is in accordance with the very little number of debris observed between the rods. As an out-of-phase loading leads to an increase in the number of slip systems, we can estimate the corresponding increase in the density of geometrically necessary dislocations. Such an increase in the dislocation density is shown on figure 3b.

Considering the expression of the shear resistance given by Calabrese and Laird (10), we find an overstrengthening of about 30 % (see (10)), which seems to be reasonable beside our experimental results (table 2). With such an approach, we can expect a great number of debris between the rods, because of the interactions between the dislocations of several systems ; in fact, the microstructural observations reveal more numerous loops in the interrod space under non proportional loading.

Damage development

Experimental results

The evolution of the maximum Von Mises equivalent stress of each cycle (σ_{VMmax}) as a function of the accumulated plastic strain p is shown on figure 6, for the two heat treatments.

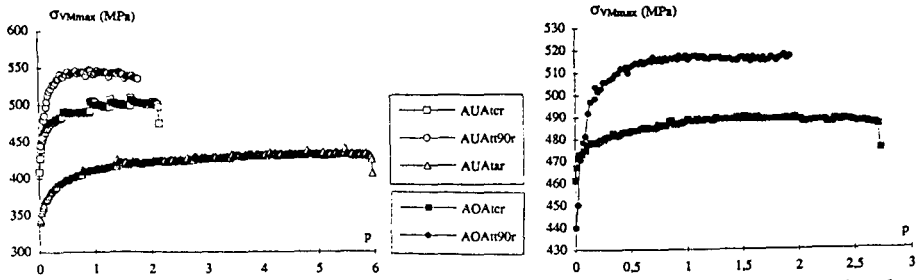


Figure 6. Evolution of the maximum equivalent stress as a function of the accumulated plastic strain, until the fracture
 AUAtcr : U.A. state, tension test AUAtt90r : U.A. state, out-of-phase tension-torsion test
 AUAtar : U.A. state, reversed torsion test
 AOAtcr : O.A. state, tension test AOAtt90r : O.A. state, out-of-phase tension-torsion test

For the two heat treatments, a nonproportional tension-torsion loading affects the cyclic stress response of the material, and the life of the specimens. As predicted by the literature (11, 12), the endurance under reversed torsion is up to three times larger than under tension.

Directional aspect of microstructural damage

For each test, the density (accumulated length) of microcracks versus orientation was measured (for more details about the experimental procedure, see (13, Ferney)). Histograms showing the angular repartition of damage around the direction perpendicular to the specimen axis (0°), at the end of the life, were obtained (figures 7 and 8).

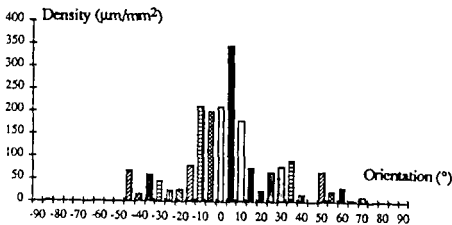


Figure 7a. U.A. state. Directional density of microcracks under tension test

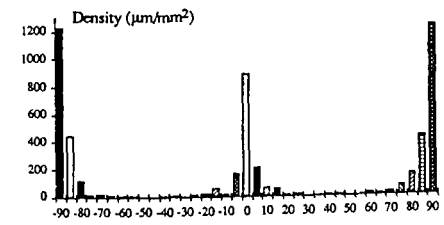


Figure 7b. U.A. state. Directional density of microcracks under reversed torsion test

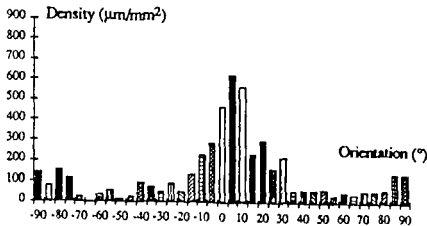


Figure 7c. U.A. state. Directional density of microcracks under out-of-phase tension-torsion test

For tension tests, cracks are present on the direction perpendicular to the specimen axis (0°), for both heat treatments (figures 7a and 8a). In the U.A. state, for the specimen tested under reversed torsion, cracks are present on both maximum plastic shear strain directions (0° and 90°). For both states, a significant increase in the microcracks density is observed for nonproportional loadings. The preferred cracking orientation along one direction is less clear, and the cracking orientation is observed along the specimen axis too (90°). In fact, for the U.A. state, there is no direction without cracking at the end of the life.

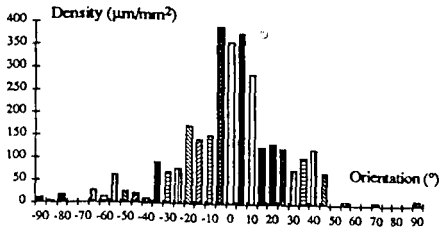


Figure 8a. O.A. state. Directional density of microcracks under tension test

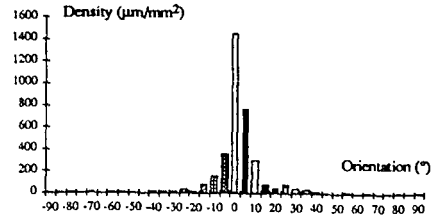


Figure 8b. O.A. state. Directional density of microcracks under out-of-phase tension-torsion test

Discussion

Tension. For tension tests, the peak value is around 0° , i.e. the direction perpendicular to the tensile stress. This result is in accordance with those of Jacquelin et al. (11) and Doquet et al. (12). Forsyth (14) has identified two distinct stages of crack growth. In Stage I, cracking proceeds along slip planes oriented in the directions of high shear stress. Subsequent Stage II growth, which is non crystallographic, occurs perpendicular to the applied tensile stress. The presence of cracks at 0° suggests that under tensile loading, Stage I not occur, and be completely replaced by Stage II. In fact, microstructural observations in SEM (figure 9) were made after the test. On figure 9, it is shown that cracking occurs by fracture of $Al_{12}(Fe, Mn)_3Si_2$ intermetallic compounds, fact which is in accordance with previous results (1). Then, cracking proceeds along directions at 45° , which are the maximum shear strain directions.

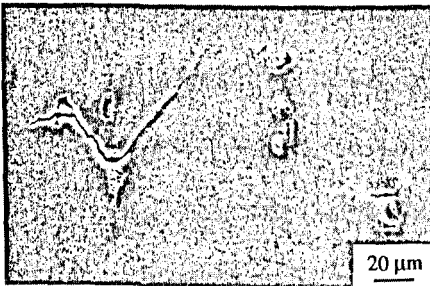


Figure 9. U.A. state. SEM. Micrograph of the outer surface of the specimen subjected to tension (the specimen axis is vertical)

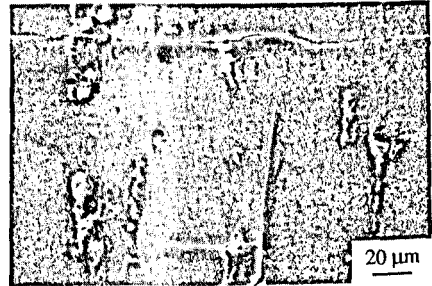


Figure 10. U.A. state. SEM. Micrograph of the outer surface of the specimen subjected to reversed torsion (specimen axis vertical)

So, we can conclude that, under a tensile loading, cracking in the 2024 proceeds first in the direction perpendicular to the normal stress, with fracture of the intermetallic compounds. Subsequent Stage I occurs in the planes bearing the largest shear strain amplitude.

Reversed torsion. In torsion, cracks usually grow along the maximum shear planes (11, 12, 15), fact which suggests that under these conditions, Stage II growth be completely replaced by Stage I even at short lives. For the 2024, cracks are present on both maximum plastic shear strain directions (figure 10), observation which is in accordance with the literature results. For the direction perpendicular to the specimen axis, cracking is transgranular. However, for the direction parallel to the specimen axis, our observations reveal that cracking seems to be intergranular.

As predicted by the literature, under reversed torsion loading, the cracking in the 2024 U.A. is essentially governed by the shear strain amplitude undergone by each plane (Stage I).

Out-of-phase tension-torsion. Under non proportional loadings, the cracking is usually not only based on the maximum shear strain. Because of the rotation of principal axes during nonproportional loading, the maximum shear strain direction is more evenly distributed among all possible directions, and the normal stress should be considered in most of cases (16, 17, 15). For the 2024, whatever the heat treatment, the damage development is more important under nonproportional loadings, and cracks tend to grow in all directions. For the O.A. state, the peak value is around 0° , and for the U.A. state, the peak values are around 0° and 90° . These directions are the two maximum shear strain directions. As more crack length has been observed around the 0° direction than around the 90° direction, there is an important normal stress influence. These results are in accordance with the ones of Kanazawa et al. (17), and Bérard et al. (15).

In accordance with the literature results, during out-of-phase biaxial fatigue tests, Stage I fatigue cracks initiate on that plane of maximum shear strain range which experiences the greatest amplitude of normal strain.

Conclusion

Under uniaxial loading, the strengthening is highly dependant of the deformation modes. In the U.A. state, the isotropic component is negative and increasing during the test, in accordance with the presence of prismatic loops, whereas in the O.A. state, it is positive and constant, in accordance with the structure of interface dislocations. Under nonproportional loading, the overstrengthening originates mainly from the isotropic component, because of an increase in slip multiplicity.

For a given equivalent plastic strain amplitude, the endurance is reduced by a nonproportional loading and a significant increase in the microcracks density is observed. For most of loadings, the orientation of the microcracks corresponds to the planes bearing the largest shear strain amplitude ; but there is a normal stress influence too, particularly for the out-of-phase loading.

References

1. L. Hautefeuille-Beylat, Ph. D. thesis, Université de Technologie de Compiègne, (1991).
2. C. Calabrese and C. Laird, Mat. Sci. Eng. **13**, (1974), 159.
3. A.H. Cottrell, Dislocations and Plastic Flow in Crystals, (Oxford Univ. Press, London, 1953), 111.
4. D. Kuhlmann-Wilsdorf and C. Laird, Mat. Sci. Eng. **37**, (1979), 111.
5. A. Abdul-latif, M. Clavel, V. Ferney and K. Saanouni, ASME J. of Eng. Mat. and Tech. **116**, (1994), 35.
6. L. Hautefeuille and M. Clavel, Scripta Metall. **22**, (1988), 1383.
7. M.F. Ashby, Strengthening Methods in Crystals, A. Kelly and R.B. Nicholson, (Elsevier, New York, 1971), 137.
8. P. Pilvin, Ph. D. thesis, Université de Paris VI, (1990).
9. V.F. Kocks and T.J. Brown, Acta Metall. **14**, (1966), 87.
10. V. Ferney, L. Hautefeuille, M. Clavel, Revue de Métallurgie **7-8**, (1991) 441.
11. B. Jacquelin, F. Hourlier and A. Pineau, Multiaxial Fatigue, ASTM STP 853, ed. K. J. Miller and M. W. Brown, (Am. Soc. for Test. and Mat., Philadelphia, 1985), 285.
12. V. Doquet and A. Pineau, Fatigue Under Biaxial and Multiaxial Loading, ESIS10, ed. K. Kussmaul, D. McDiarmid, and D. Socie, (Mech. Eng. Publications, London, 1991), 81.
13. V. Ferney, Ph. D. thesis, Université de Technologie de Compiègne, (1994).
14. P. J. E. Forsyth, Proc. Symp. on Crack Propagation, (Cranfield, England), (1961).
15. J.Y. Bérard, S.D. Antolovich and D. L. McDowell, Revue de Métallurgie-CIT **6**, (1991) 557.
16. M. W. Parsons, K. J. Pascoe, Mat. Sci. Eng. **22**, (1976), 31.
17. K. Kanazawa, K. J. Miller, M. W. Brown, ASME J. Eng. Mater. Technol. **99**, (1977), 222.